

Dynamics of Colloidal Particles in Soft Matters

Takeaki ARAKI^{*)} and Hajime TANAKA^{**)}

Institute of Industrial Science, University of Tokyo, Tokyo 153-8505, Japan

We developed numerical methods for studying the dynamics of colloidal particles suspended in complex fluids. It is essential to employ a coarse-grained model for studying slow dynamics of these systems. Our methods are based on the “fluid particle dynamics (FPD)” method, which we have developed to deal with hydrodynamic interactions in colloidal systems in an efficient manner. We regard a solid particle as an undeformable fluid one. It has a viscosity much higher than the solvent, which smoothly changes to the solvent viscosity at the interface. This method allows us to avoid troublesome boundary conditions to be satisfied on the surfaces of mobile particles. Since we express the spatial distribution of colloids as a continuum field, we can easily introduce the order parameter describing a complex solvent, e.g., ion distribution for charged colloids, director field for nematic liquid crystal, and concentration for phase-separating binary fluid. Then we solve coupled dynamic equations of three relevant parameters, i.e., particle positions, flow field, and the order parameter. We demonstrate a few examples of such simulations.

§1. Introduction

Recently, suspensions of colloids or nanoparticles in complex fluids have attracted considerable attentions from both the fundamental and practical viewpoints.^{1)–11)} For example, particles dispersed in a nematic liquid crystal have an anisotropic and non-pairwise interaction mediated by the elastic field of a nematic solvent.^{1)–3)} This peculiar interaction yields an unusual soft solid made of colloid-liquid crystal composites.⁴⁾ It was also shown that neutrally wettable particles in a phase-separated binary fluid are strongly bound on the interface of the two phases, which leads to a glassy state of Pickering emulsion.⁵⁾

Numerical simulations are very powerful and useful tools to study the dynamic properties of these colloidal systems. However, there remain some difficulties originating from multi-scale hierarchies in time and space. For example, if we try to simulate an aqueous suspension of colloidal particles of 100 nm without coarse-graining, we have to solve the dynamics of all constituents including more than 10^{12} water molecules. So, it is very difficult to reach even the Brownian diffusion time of a particle, $\tau_B \sim 5$ ms. To overcome this difficulty, a number of numerical schemes have been developed: Lattice Boltzmann,^{12)–16)} dissipative particle dynamics,¹⁷⁾ stochastic rotational dynamics,^{18),19)} fluid particle dynamics (FPD)^{20),21)} and smoothed profile method.^{22),23)} A common feature among these simulation methods is that small, fast solvent molecules are treated in a coarse-grained manner. In such simulations, coupled dynamics of relevant variables, particle positions, flow field and order parameter(s) describing the complex fluid are numerically solved.

^{*)} Present address: Department of Physics, Kyoto University.

E-mail: araki@scphys.kyoto-u.ac.jp

^{**)} E-mail: tanaka@iis.u-tokyo.ac.jp

In this paper, we show efficient numerical simulation methods for studying many particle dynamics of colloids in soft matters. Our method is based on fluid particle dynamics (FPD), which we developed to simulate the hydrodynamic interactions between colloidal particles in a simple liquid.^{20),21)} The method was used to study the structural formation of colloids undergoing phase separation.^{20),21),24)} The most difficult problem in simulating colloids immersed in a solvent is the hydrodynamic solid-fluid boundary conditions, which must be satisfied on the surfaces of all moving particles. In FPD, we treat a solid particle as an undeformable fluid having larger viscosity than the solvent. A smooth profile between a colloidal particle and the solvent makes us free from the boundary conditions, as explained later. In the limit of larger viscosity ratio between the outside and inside of the particle, the flow field inside the particle becomes homogeneous so as to reduce viscous dissipation, and thus the fluid particle can be regarded as the solid particle. In addition to this numerical efficiency for calculating hydrodynamic interactions, FPD method has another merit, i.e., an applicability to colloid-soft matter complexes. Since we solve the solvent as a continuum field, we can easily introduce order parameters relevant to various soft matter. Below we present the details of our FPD method and three applications.

§2. Fluid particle dynamics method

Here we briefly explain our FPD method.^{20),21)} The key of our FPD method is to treat a solid colloidal particle as an undeformable fluid particle, which has a smooth interface. We express i -th fluid particle using a hyperbolic tangent function as $\phi_i(\mathbf{r}) = [\tanh\{(a - |\mathbf{r} - \mathbf{r}_i|)/\xi\} + 1]/2$, where a is the particle radius and ξ is the interfacial width (see Fig. 1(a)). For the spatial distribution of particles given by $\{\mathbf{r}_i\}$, the viscosity field can be expressed as $\eta(\mathbf{r}) = \eta_s + \sum_i(\eta_c - \eta_s)\phi_i(\mathbf{r})$, where η_s is the viscosity of the fluid surrounding particles and η_c is the viscosity inside the particle. Note that η can be a tensor in the case of an anisotropic solvent. Then the time evolution of \mathbf{v} is described by the following Navier-Stokes equations,

$$\rho \left(\frac{\partial}{\partial t} + \mathbf{v} \cdot \nabla \right) \mathbf{v} = \mathbf{F} - \nabla p + \nabla \cdot \eta \{ \nabla \mathbf{v} + (\nabla \mathbf{v})^T \}, \quad (2.1)$$

where ρ is the density. In the above, we assume that the density of colloidal particles is the same as that of a liquid, namely, ρ is homogeneous in space. Pressure p is determined to satisfy the incompressible condition $\nabla \cdot \mathbf{v} = 0$. $\mathbf{F}(\mathbf{r})$ is a force field given by $\mathbf{F}(\mathbf{r}) = \mathbf{F}'(\mathbf{r}) + \sum_i \mathbf{F}_i^{(0)} \phi_i(\mathbf{r})/V$, where $V = \int d\mathbf{r} \phi_i(\mathbf{r})$. $\mathbf{F}_i^{(0)}$ is a direct body force on i -th particle. To avoid the overlap of particles, we use the repulsive part of the Lennard-Jones potential as the body force: $\mathbf{F}_i^{(0)} = \sum_{j \neq i} \mathbf{f}(\mathbf{r}_i - \mathbf{r}_j)$. Here $\mathbf{f}(\mathbf{r}) = -(\partial/\partial \mathbf{r})U_0[(2a/|\mathbf{r}|)^{12} - (2a/|\mathbf{r}|)^6]$ with $|\mathbf{r}| < 2^{7/6}a$, where U_0 is the strength of this steric repulsion. And $\mathbf{F}'(\mathbf{r})$ means the force field coming from the free energy associating the soft matter under the consideration (see below). The time evolution of the position of particle i , \mathbf{r}_i , is described by the average fluid velocity inside the

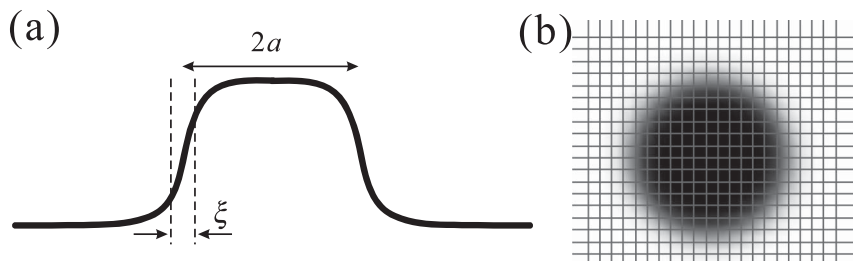


Fig. 1. Description of a particle in the FPD method. (a) Profile of a smooth particle of the radius a and width ξ . (b) Mapping of the particle onto a square lattice.

particle,

$$\frac{d}{dt}\mathbf{r}_i = \frac{1}{V} \int d\mathbf{r} \mathbf{v}(\mathbf{r}) \phi_i(\mathbf{r}). \quad (2.2)$$

This is the framework of the original FPD model. It should be noted that the fluid particle approximation becomes exact in the limit of $\eta_c/\eta_s \rightarrow \infty$ and $\xi/a \rightarrow 0$.²⁵⁾

We discretize the coarse-grained variables $\phi_i(\mathbf{r})$ and $\mathbf{v}(\mathbf{r})$ into the staggered lattice by the interface width ξ (see Fig. 1(b)). And the hydrodynamic flow is calculated by solving Eq. (2.1) with Makers and Cell (MAC) method.²⁶⁾ Particle positions are updated by solving Eq. (2.2) in an off-lattice space with an explicit Euler scheme. In order to reduce the inertia effect, we iterate Eq. (2.1), so as to satisfy $\langle |\rho D\mathbf{v}/Dt| \rangle / \langle |\mathbf{F}| \rangle < Re$, without updating particle positions. Here Re is a non-dimensional parameter of the order of 10^{-2} .

§3. Particle dynamics in soft matters

We introduced three types of order parameters into the coarse-grained solvent. By solving the dynamic equations for the order parameters simultaneously, we can simulate the coupled dynamics of colloids and soft matters. We simulated three different soft matter complexes in a common way: (i) charged colloidal dispersion in an ionic solution,^{27),28)} (ii) particles in nematic liquid crystal^{29),30)} and (iii) particles in a phase-separating binary fluid.^{31),32)} In the following, we will show some results of our simulations.

3.1. Charged colloidal system

First we show results of a charged colloidal system, where ions are solved in water.^{27),28)} We denote the concentration and valence of ion species α by C_α and z_α , respectively. We express the charge density localized in the surface region of particle i as $\rho_i(\mathbf{r}) = Ze|\nabla\phi_i(\mathbf{r})|^2 / \int d\mathbf{r} |\nabla\phi_i(\mathbf{r})|^2$, where Z is the number of charges on a particle. The total charge density is then expressed as $\rho_e(\mathbf{r}) = \sum_i \rho_i(\mathbf{r}) + \sum_\alpha ez_\alpha C_\alpha(\mathbf{r})$. In this paper, we consider a system composed of positively charged colloids and two types of ions (+ and -). The charge neutrality condition is then given by $\int d\mathbf{r} (z_+ C_+ + z_- C_- + Z\phi/V) = 0$. The salt concentration C_s is given by the spatially averaged value of C_+ . The electrostatic potential Ψ satisfies the Poisson

equation, $\epsilon_r \epsilon_0 \nabla^2 \Psi = -\rho_e$, where ϵ_r is the relative dielectric constant and ϵ_0 is the permittivity of vacuum. The time evolution of the ion concentration field C_α is described by³³⁾

$$\left(\frac{\partial}{\partial t} + \mathbf{v} \cdot \nabla \right) C_\alpha = -\nabla \cdot \mathbf{J}_\alpha, \quad (3.1)$$

where $\mathbf{J}_\alpha = -D_\alpha C_\alpha \nabla \mu_\alpha / k_B T$ is the flux of ion α induced by the gradient of the chemical potential μ_α , where D_α is the diffusion constant of ion α , k_B is Boltzmann's constant, and T is the temperature. The effective chemical potential μ_α is expressed as $\mu_\alpha = k_B T \ln C_\alpha + e Z_\alpha \Psi + k_B T \chi_\alpha C_\alpha \sum_i \phi_i$. Here the first term comes from the translational entropy of ions, the second one from the electrostatic contribution, and the third one from the penalty for the ions entering the inner region of the particles. χ_α is a parameter describing the interaction between the ions and the particle, which is artificially introduced to prevent the ions from penetrating into the particles. The force field \mathbf{F}' in Eq. (2.1) stems from the electrostatic interaction and is expressed as $\mathbf{F}' = -\rho_e (\nabla \Psi - \mathbf{E})$. \mathbf{E} is an external electric field. Note that the direct force $\mathbf{F}_i^{(0)}$ should not contain the Coulomb interaction since that is already included in \mathbf{F}' . By setting $\xi = b e^2 / (4\pi \epsilon_0 k_B T)$, the ion concentration is also described in the lattice space, where b is a numerical scaling factor ($b \lesssim 0.2$ in our simulations).

Figure 2(a) shows the simulated counter ion cloud around a single charged particle. Here, the electric field is applied vertically and the particle is moving downward. The cloud of counter ions is distributed asymmetrically, and this asymmetry causes the relaxation effect on the electrophoretic motion. The spatial distribution of ions at rest is characterized by the Debye-Hückel parameter $\kappa = \sqrt{2z^2 e^2 C_s / (\epsilon_r \epsilon_0 k_B T)}$. Our simulation is consistent with the analytical form of the ion distribution within numerical accuracy. Figure 2(b) plots the profiles of the internal electric field Ψ along the direction of the external field going through the center of a particle. Ψ at the particle surface corresponds to the zeta potential. Here, the particle is drifting toward the left. When the salinity is low (small κa), the electric field is almost symmetric around the particle. By adding salt, the profile of Ψ becomes sharper and more asymmetric. $-\nabla \Psi$ inside the particle represents the induced dipole. Interestingly, the direction of the dipole is inverted at the critical salinity ($\kappa a \approx 0.5$ in this case). This means that the polarization coefficient of the particle is changed from positive to negative with an increase in κa . The force on the counter ion is opposite to that on the particle. For a small κa , the ion cloud is slightly shifted to the backward as shown in Fig. 2(a). The induced dipole is toward the same direction of the applied electric field. For a large κa , on the other hand, counter ions are accumulated at the front of the drifting particle. Thus the induced dipole is opposite to the direction of the electric field. It is known that this inversion of the polarization is characterized by the so-called Dukhin number,³⁴⁾ which is the ratio between the conductivity of the ions in the bulk and that along the surface. The Dukhin number is a function of ζ and κ . Our simulation is consistent with the theoretical prediction.³⁵⁾

One of the merits of our numerical method is that we can study many body effects in the dynamical behavior of a system. Figure 3 shows the snapshot of a 2D colloidal dispersion in a non-equilibrium condition. At $t = 0$, we start to apply the

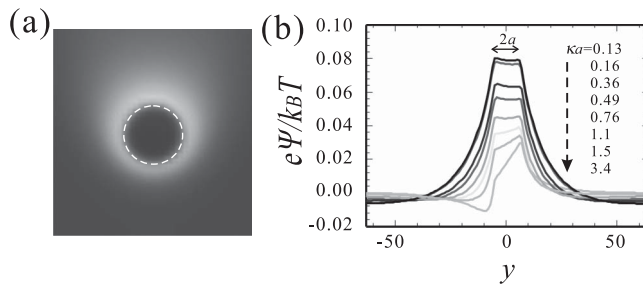


Fig. 2. Electrophoresis of a single charged particle. (a) Simulated distribution of the counter ion. The circle of the broken line represents the particle. (b) Profiles of the electric potential Ψ around a driven particle.

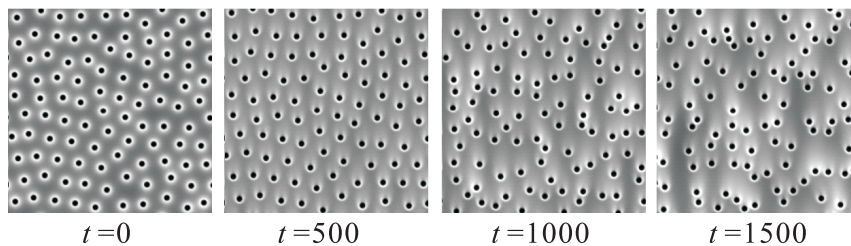


Fig. 3. Simulated pattern evolution of a colloidal suspension under an electric field. At $t = 0$, we start to apply the field.

field to the system. At the rest ($t < 0$), the charged particles repulsively interact each other, so they are distributed homogeneously with hexagonal local positional order. Under a weak field, particles move along the field rather homogeneously (not shown here). Under a strong field, dynamical coupling of particle motion leads to chaotic behavior. The coupling is produced by the hydrodynamic interaction between particles, as in the sedimentation of non-Brownian particles.³⁶⁾ In contrast to charge-free particles, the hydrodynamic interaction can be reduced by salt as in the case of electrostatic interaction.³⁷⁾ This opens up a possibility of optimization of the electrophoretic separation of particles and biomolecules, which was discussed in detail elsewhere.²⁸⁾

3.2. Particles immersed in nematic liquid crystal

To simulate particles suspended in a nematic solvent,^{29),30)} we introduce a nematic order parameter Q_{ij} ³⁸⁾ into the solvent. The free energy of a nematic liquid crystal is given as

$$\mathcal{F}\{Q_{ij}, \phi\} = \int d\mathbf{r} \left\{ f(Q_{ij}, \phi) + \frac{K_1}{2} (\partial_k Q_{ij})^2 + \frac{K_2}{2} (\partial_i Q_{ij})^2 - W \xi Q_{ij} \partial_i \phi \partial_j \phi - E_i E_j Q_{ij} \right\}, \quad (3.2)$$

where repeated indices are implicitly summed over. The first term of Eq. (3.2) is the free energy of a bulk nematic phase given by $f(Q_{ij}, \phi) = -\frac{1}{2}A(1-2\phi)Q_{ij}Q_{ji} - \frac{1}{3}BQ_{ij}Q_{jk}Q_{ki} + \frac{1}{4}C(Q_{ij}Q_{ji})^2$, where B and C are the positive constants. A is negative and positive above and below the transition, respectively. Note that even below the transition, the inside of particles remains negative since $A(1-2\phi) < 0$. The second and third terms of Eq. (3.2) represent the Frank elasticity: K_1 and K_2 are their elastic moduli. The fourth term is the anchoring energy of the nematic phase at the particle surface: W is the energetic cost of the anchoring per unit area. The fifth term represents a coupling between an external (electric or magnetic) field E_i and the director field.

Time evolution of Q_{ij} and \mathbf{v} is then described by

$$\frac{DQ_{ij}}{Dt} = Q_{ik}\Omega_{kj} - \Omega_{ik}Q_{kj} + \frac{H_{ij}}{\mu_1} + \frac{\mu_2 A_{ij}}{2\mu_1} + \lambda_{ij}, \quad (3.3)$$

$$\begin{aligned} \rho \frac{Dv_i}{Dt} = & F_i - \phi \partial_i \mu + Q_{jk} \partial_i H_{jk} \\ & + \partial_j (H_{ik} Q_{kj} - Q_{ik} H_{kj}) - \partial_i p + \partial_j \Sigma_{ij}. \end{aligned} \quad (3.4)$$

Here, $\mu = \frac{\delta \mathcal{F}}{\delta \phi}$ and $H_{ij} = -\left\{ \frac{\delta \mathcal{F}}{\delta Q_{ij}} - \frac{1}{3} \delta_{ij} \delta_{kl} \frac{\delta \mathcal{F}}{\delta Q_{kl}} \right\}$ are the effective chemical potential for particle concentration ϕ and the molecular force field for nematic order Q_{ij} , respectively.³⁸⁾ $A_{ij} = \frac{1}{2}(\partial_i v_j + \partial_j v_i)$ and $\Omega_{ij} = \frac{1}{2}(\partial_i v_j - \partial_j v_i)$ are symmetric and asymmetric velocity gradient tensors. $\Sigma_{ij} = \beta_1 Q_{ij} Q_{kl} A_{kl} + \left(\beta_4(\phi) - \frac{\mu_2^2}{2\mu_1} \right) A_{ij} + \frac{\beta_5 + \beta_6}{2} (Q_{ik} A_{kj} + A_{ik} Q_{kj}) - \frac{\mu_2}{2\mu_1} H_{ij}$ is a mechanical stress tensor for the flow field. $\beta_1, \beta_4, \beta_5, \beta_6, \mu_1,$ and μ_2 are constants having a dimension of viscosity. In the spirit of FPD, the shear viscosity depends on the particle configuration as $\beta_4 = \bar{\beta}_4 + \Delta\beta_4\phi(\mathbf{r})$.²⁰⁾ Here $\bar{\beta}_4$ and $\bar{\beta}_4 + \Delta\beta_4$ correspond to the shear viscosities outside and inside a fluid particle, respectively. λ_{ij} in Eq. (3.3) is the thermal fluctuation for Q_{ij} . Here we impose the thermal fluctuation λ_{ij} only for Q_{ij} for simplicity. We assume that the density of a colloidal particle is the same as that of a host fluid; thus, the density ρ is constant. The length, time, and force are normalized by the characteristic length $\Xi = \sqrt{K_1/A}$, characteristic rotational time $t_Q = \mu_1 \Xi^2 / K_1$, and elastic modulus K_1 , respectively.

In this subsection, we employ the following parameters: the Reynolds number $Re = \frac{\rho K_1}{\eta \mu_1} = 0.02$, the ratio between the two Frank elasticity moduli $K_2/K_1 = 0.5$, $B/A = 25$, $C/A = 20$, and $\tilde{W} = 10$ (strong homeotropic anchoring). We denote the degree of orientational order of the nematic phase as $Q_0 = \frac{B + \sqrt{B^2 + 24AC}}{6C}$. The ratios between the viscosities of the nematic phase are as follows: $\mu_1 Q_0^2 / \eta = 0.65$, $-\frac{\mu_2}{2\mu_1 Q_0} = 2.0$, $\frac{(\beta_5 + \beta_6) Q_0}{2\eta} = 0.06$, and $\beta_1 Q_0^2 / \eta = 0.1$, where $\eta = \bar{\beta}_4 - \frac{\mu_2^2}{2\mu_1}$ is a viscosity for usual shear flow.

Particles suspended in a nematic liquid crystal interact to each other via the elastic field of the anisotropic solvent. This interaction leads to some ordered structure of intrinsically non-interacting particles.^{1),3)} When the director field tends to be normal to the particle surface (homeotropic anchoring), two types of defect structures are formed depending on the particle size and the external field.³⁾ Saturn-ring-like defect

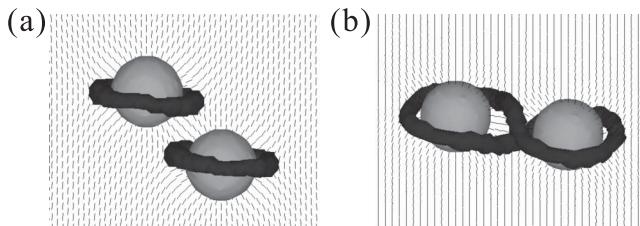


Fig. 4. Stable and metastable configurations of a particle pair in a nematic liquid crystal, due to a quadrupole symmetry (a) and a single stroke disclination (b).

is one of the two possible configurations. A particle accompanying the Saturn-ring defect has a quadrupole symmetry. Thus, it is expected that they interact to others with the quadrupole symmetry^{2),3)} as shown in Fig. 4(a). In addition to this pairwise interaction, we found a new type of interaction between particles with Saturn-ring defects. Figure 4(b) shows the defect configuration around a pair of particles. Here a single disclination line is shared by the two particles and has a shape of the figure of eight. It tends to shrink to reduce the elastic energy and binds the particles, but cannot cross itself due to the large energy barrier associated with the topological change of the defect. This ‘figure of eight’ structure has higher energy than that of quadrupole interaction (Fig. 4(a)), so that it is not a stable configuration. Since the energy barrier between these two configurations is higher than thermal fluctuation, however, it can exist for an observable period.³⁹⁾ The mechanism is discussed in detail elsewhere.²⁹⁾

3.3. Phase-separating binary fluids containing particles

Next we show results of particles suspended in binary fluid mixtures.^{5),8)-10),16)} Generally, the particle surface favors one of the components (wetting effects). Beyens and Estève found this wetting interaction leads to the flocculation of colloids while approaching the phase-separation temperature even in a one-phase region.⁸⁾ One of us (H. T.) reported the addition of particles can be used to control the morphology of phase-separation patterns.⁹⁾ Even when the two components equally wet particles, particles tend to sit on the interface between the two coexisting phases. This leads to an intriguing glassy behavior of the system: glassy Pickering emulsions.^{5),16)}

The coarse-grained variable relevant for the physical description of phase-separation dynamics of a fluid mixture is the concentration field ψ . We employ the following free energy functional for a binary mixture containing particles:

$$\mathcal{F}\{\psi, \phi\} = \int d\mathbf{r} [f(\psi) - W\xi\psi|\nabla\phi|^2 - \chi\Delta\psi^2\phi]. \quad (3\cdot5)$$

The first term of the right hand side (r.h.s.) of Eq. (3·5) corresponds to the Ginzburg-Landau-type mixing free energy of a binary mixture with $f(\psi) = \tau\psi^2/2 + u\psi^4/4 + K|\nabla\psi|^2/2$, where τ , u and K are constants (note that $\tau > 0$ before quench, $t < 0$). The second term stands for the wetting interaction between a binary mixture and a particle surface (represented as $|\nabla\phi|^2$ in our scheme). W represents the strength of

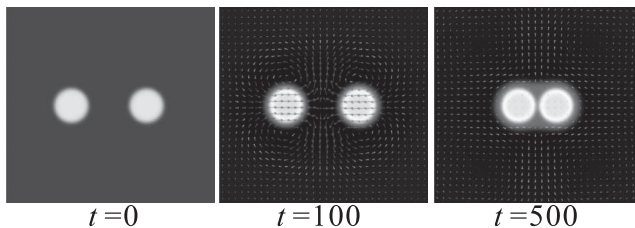


Fig. 5. Time evolution of a particle pair in a phase separating binary fluid. At $t = 0$, we quench the system from the one-phase to the two-phase region.

this wetting interaction; here $W > 0$ means that the phase of $\psi > 0$ favors a particle surface. The third term is introduced such that the concentration field inside each particle becomes $\psi \approx \bar{\psi}$, where $\chi (> 0)$ is its coupling constant and $\bar{\psi}$ is the average of ψ . Note that $\Delta\psi = \psi - \bar{\psi}$.

The time development of ψ is described by

$$\frac{\partial\psi}{\partial t} = -\mathbf{v} \cdot \nabla\psi + L\nabla^2\mu, \quad (3.6)$$

where μ is the chemical potential defined as $\mu = \delta\mathcal{F}/\delta\psi$. L is the kinetic coefficient, which is assumed to be independent of ψ . The osmotic pressure is introduced by $\mathbf{F}' = -\phi\nabla\mu$ in the hydrodynamic equation (2.1). The characteristic length and time of phase separation are given by $\ell = (-K/\tau)^{1/2}$ and $t_\ell = \ell^2/L$, respectively. To fix i -th particle around a position \mathbf{r}_i^f by a spring, we add $\kappa(\mathbf{r}_i - \mathbf{r}_i^f)$ to $\mathbf{F}_i^{(0)}$, κ is a spring constant. We set the parameters as $u = 1$, $K = 1$ and $L = 1$. And interface width of the smooth particle is set to $\xi = \ell$. The other parameters are set as $\xi = 1$, $\epsilon = 1$, $\chi = 2$, and $W = 8$.

Figure 5 demonstrates that a strong attractive interaction acts on a particle pair in a phase-separating binary fluid mixture. In the early stage of phase separation, the component more wettable to particles diffuses toward the particle surfaces to cover them. Since the diffusion flux is isotropic for an isolated particle, the osmotic force is canceled by pressure under the incompressible condition and thus does not cause hydrodynamic flow. When two particles are placed nearby, on the other hand, the diffusion flux becomes anisotropic around each particle because of the depletion of the more wettable phase between the particles. The osmotic force can no longer be canceled by pressure, and pushes a particle to the other. We showed that this wetting-induced depletion force can be stronger than a van der Waals interaction and a capillary force,³³⁾ which is induced by the interface tension. The details of the mechanism were discussed elsewhere.³¹⁾

§4. Summary

We developed new numerical methods for studying colloids or nanoparticles suspended in complex fluids, on the basis of FPD method, which can deal with hydrodynamic interaction between colloidal particles without suffering from complex hydrodynamic boundary conditions. We applied the methods to simulate the three

types of soft matter complexes: (i) charged colloidal dispersion in an ionic solution, (ii) particles in nematic liquid crystal, and (iii) particles in a phase-separating binary fluid. In all the examples, dynamical couplings among the relevant variables, particles, flow, and the order parameter, lead to very rich and interesting behavior, which we showed are physically reasonable. So our method may be used to explore new interesting static and dynamic features in non-equilibrium soft matter.

Acknowledgements

This work was supported by KAKENHI's, a Grant-in-Aid for Scientific Research on Priority Area ("Soft Matter Physics") and a Grant-in-Aid for Creative Scientific Research from the Ministry of Education, Culture, Sports, Science and Technology of Japan.

References

- 1) P. Poulin, H. Stark, T. C. Lubensky and D. A. Weitz, *Science* **275** (1997), 1770.
- 2) R. W. Ruhwandl and E. M. Terentjev, *Phys. Rev. E* **55** (1997), 2958.
- 3) H. Stark, *Phys. Rep.* **351** (2001), 387.
- 4) S. P. Meeker, W. C. K. Poon, J. Crain and E. M. Terentjev, *Phys. Rev. E* **61** (2000), R6083.
- 5) B. P. Binks and J. H. Clint, *Langmuir* **18** (2002), 1270.
- 6) S. Asakura and F. Oosawa, *J. Chem. Phys.* **22** (1955), 1255.
- 7) W. C. K. Poon, *J. of Phys.: Cond. Mat.* **14** (2002), R859.
- 8) D. Beysens and D. Estève, *Phys. Rev. Lett. D* **54** (1985), 2123.
- 9) H. Tanaka, A. J. Lovinger and D. D. Davis, *Phys. Rev. Lett.* **72** (1994), 2581.
- 10) H. Tanaka, *J. of Phys.: Cond. Mat.* **13** (2001), 4637.
- 11) A. Stradner, H. Sedgwick, F. Cardinaux, W. C. K. Poon, S. U. Egelhaaf and P. Schurtenberger, *Nature* **432** (2004), 492.
- 12) A. J. C. Ladd, *J. Fluid. Mech.* **271** (1994), 285.
- 13) J. Horbach and D. Frenkel, *Phys. Rev. E* **64** (2001), 061507.
- 14) A. Chatterji and J. Horbach, *J. Chem. Phys.* **122** (2005), 184903.
- 15) V. Lobaskin, B. Dünweg, M. Medebach, T. Pelberg and C. Holm, *Phys. Rev. Lett.* **98** (2007), 176105.
- 16) K. Stratford, R. Adhikari I. Pagonabarraga, J. C. Desplat and M. E. Cates, *Science* **309** (2005), 2198.
- 17) V. Lobaskin, B. Dünweg and C. Holm, *J. of Phys.: Cond. Mat.* **16** (2004), S4063.
- 18) A. Malevanets and R. Kapral, *J. Chem. Phys.* **110** (1999), 8605.
- 19) J. T. Padding, A. Wysocki, H. Löwen and A. A. Loius, *J. of Phys.: Cond. Mat.* **17** (2005), S3393.
- 20) H. Tanaka and T. Araki, *Phys. Rev. Lett.* **85** (2000), 1338.
- 21) H. Tanaka and T. Araki, *Chem. Eng. Sci.* **61** (2006), 2108.
- 22) R. Yamamoto, *Phys. Rev. Lett.* **87** (2001), 075502.
- 23) K. Kim, Y. Nakayama and R. Yamamoto, *Phys. Rev. Lett.* **96** (2006), 208302.
- 24) H. Tanaka and T. Araki, *Europhys. Lett.* **79** (2007), 58003.
- 25) Y. Fujitani, *J. Phys. Soc. Jpn.* **75** (2006), 013401.
- 26) F. H. Harlow and J. E. Welch, *Phys. Fluids* **8** (1965), 2182.
- 27) H. Kodama, K. Takeshita, T. Araki and H. Tanaka, *J. of Phys.: Cond. Mat.* **16** (2004), L115.
- 28) T. Araki and H. Tanaka, *Europhys. Lett.* **82** (2008), 18004.
- 29) T. Araki and H. Tanaka, *Phys. Rev. Lett.* **97** (2006), 127801.
- 30) T. Araki and H. Tanaka, *J. of Phys.: Cond. Mat.* **18** (2006), L193.
- 31) T. Araki and H. Tanaka, *J. of Phys.: Cond. Mat.* **20** (2008), 072101.
- 32) T. Araki and H. Tanaka, *Phys. Rev. E* **73** (2006), 061506.
- 33) R. J. Hunter, *Foundations of Colloid Science*, 2nd edition (Oxford University Press, Ox-

- ford, 2001).
- 34) S. S. Dukhin, *Adv. Colloid Interface. Sci.* **44** (1993), 1.
 - 35) V. N. Shilov, A. V. Delgado, E. Gonzalez-Caballero, J. Horno, J. J. Lopez-Garcia and C. Grosse, *J. Colloid Interface Sci.* **232** (2000), 141.
 - 36) R. E. Caflisch and J. H. C. Luke, *Phys. Fluids* **28** (1985), 759.
 - 37) D. Long and A. Ajdari, *Eur. Phys. J. E* **4** (2001), 29.
 - 38) P. G. de Gennes and J. Prost, *The Physics of Liquid Crystals* (Clarendon Press, Oxford, 1993).
 - 39) M. Ravnik, M. Skarabot, S. Žumer, U. Tkalec, I. Roberaj, D. Babic, N. Osterman and I. Musevic, *Phys. Rev. Lett.* **99** (2007), 247801.